Food Research International 107 (2018) 41–47

Contents lists available at ScienceDirect

Food Research International

journal homepage: www.elsevier.com/locate/foodres

Food grade microemulsion systems: Sunflower oil/castor oil derivative-ethanol/water. Rheological and physicochemical analysis

Noelia Mori Cortés[a], Gabriel Lorenzo[a,b,*], Alicia N. Califano[a]

[a] Centro de Investigación y Desarrollo en Criotecnología de Alimentos (CIDCA), Facultad de Cs. Exactas, UNLP-CONICET, 47 y 116, La Plata (1900), Argentina
[b] Depto. Ingeniería Química, Facultad de Ingeniería, UNLP, Argentina

ARTICLE INFO

Keywords:
Microemulsions
Rheology
Droplet size
Viscoelasticity
Castor oil emulsifiers
Stability

ABSTRACT

Microemulsions are thermodynamically stable systems that have attracted considerable attention in the food industry as delivery systems for many hydrophobic nutrients. These spontaneous systems are highly dependent on ingredients and composition. In this work phase diagrams were constructed using two surfactants (Kolliphor RH40 and ELP), water, sunflower oil, and ethanol as cosurfactant, evaluating their physicochemical properties. Stability of the systems was studied at 25 and 60 °C, monitoring turbidity at 550 nm for over a month to identify the microemulsion region. Conductivity was measured to classify between water-in-oil and oil-in-water microemulsions. The phase diagram constructed with Kolliphor RH40 exhibited a larger microemulsion area than that formulated with Kolliphor ELP.

All formulations showed a monomodal droplet size distribution with low polydispersity index (< 0.30) and a mean droplet size below 20 nm. Systems with higher water content presented a Newtonian behavior; increasing the dispersed phase content produced a weak gel-like structure with pseudoplastic behavior under flow conditions that was satisfactorily modeled to obtain structural parameters.

1. Introduction

The design and development of different delivery systems when searching for the best option to enhance the bioavailability of nutraceutical components is an important field in food and pharmaceutical research. Currently, in food industry only a few matrices are used as delivery systems, because not only it has to be efficient but also must be food grade and relatively inexpensive (Garg, Sharma, Rath, & Goyal, 2017). Colloidal systems have been widely and actively investigated over the past four to five decades for nutrient delivery. However, nanostructure dispersions like liposomes, microemulsions, reverse micelles, and nanoemulsions appear to be an interesting option to replace the traditional delivery systems like emulsions or microspheres, that resulted unsuitable for some food matrices (Garg et al., 2017; Garti & Aserin, 2012). Particularly, microemulsions are good vehicles for solubilization and transport of water insoluble and/or oil insoluble active compounds. Microemulsions (or micellar emulsions) are macroscopically homogeneous mixtures of oil, water, and surfactant, frequently in combination with a cosurfactant. They are optically isotropic, transparent, and thermodynamically stable due their small particles size, which are in colloidal domain (Flanagan & Singh, 2006). Microemulsions have attracted considerable attention in the food and pharmaceutical industries, as they have a great capacity to solubilize hydrophobic compounds such as functional oils and vitamins and, through a rapid release in the gastrointestinal tract, improve their absorption (Janković, Djekic, Dobričić, & Primorac, 2016; Xu et al., 2016). Several authors have reported that the incorporation of a wide range of bioactive molecules in microemulsions extended its stability and offered a good opportunity for absorption, even with different solubility chemical nature, molecular weight, etc. (Callender, Mathews, Kobernyk, & Wettig, 2017; Li et al., 2017; Ma & Zhong, 2015; Rozman, Zvonar, Falson, & Gasperlin, 2009). However, the properties of these spontaneous systems are highly dependent on their ingredients and composition; they could range between various structures from droplet like swollen micelles to bi-continuous structure. Selection of surfactants is a critical process as a very low interfacial tension is required at the oil/water interface which is a fundamental requirement to form a microemulsion. Moreover, concentration of surfactant must be high enough to provide the number of surfactant molecules needed to stabilize the nano droplets. Usually, microemulsions require the presence of a cosurfactant because single chain surfactants alone are incapable to sufficiently reduce o/w interfacial tension (Lv, Zheng, & Tung, 2005). Short to medium chain length alcohols (C3-C8) are commonly added as cosurfactants; they are located between the surfactant chains and the

* Corresponding author at: 47 y 116, La Plata (1900), Buenos Aires, Argentina.
E-mail address: gabriel.lorenzo@ing.unlp.edu.ar (G. Lorenzo).

https://doi.org/10.1016/j.foodres.2018.01.073
Received 25 October 2017; Received in revised form 20 December 2017; Accepted 29 January 2018
Available online 31 January 2018
0963-9969/

continuous phase so as to increase the flexibility of the interfacial membrane. However, an excess of cosurfactant can lead to the destruction of the microemulsion due to the phenomenon of partition. This would cause migration of the surfactant from the interfacial region to the continuous phase (Warisnoicharoen, Lansley, & Lawrence, 2000). Ethanol is one of the most used cosurfactant in food systems due to its low toxicity (Fasolin, Santana, & Cunha, 2012).

As it was mentioned, the type of emulsifier plays a fundamental role in the formulation of microemulsions. Kolliphor ELP and Kolliphor RH40 (formerly known as Cremophor) are nonionic surfactants derived from castor oil, commonly used in pharmaceutical formulations to improve the bioavailability of poorly water-soluble drugs (Berthelsen et al., 2015; Hallouard, Dollo, Brandhonneur, Grasset, & Corre, 2015; Janković et al., 2016). Both surfactants are included in the list of inactive ingredients for approved drug products by the FDA (2017), and they may be incorporated in oral, intravenous, intravesical, topical, ophthalmic, or IV (infusion) pharmaceutical products without harm for individuals. However, their application in food systems has been not completely studied (El-Sayed, Chizzola, Ramadan, & Edris, 2017).

Kolliphor ELP is the commercial name of polyoxyl n castor oil (n = 35), it is a mixture of triricinoleate esters of ethoxylated glycerol with small amounts of polyethylene glycol (macrogol) ricinoleate and the corresponding free glycols. The number (n) associated with the name of the substance represents the average number of oxyethylene units in the compound. The name Kolliphor RH40 corresponds to polyoxyl 40 hydrogenated castor oil, a mixture of trihydroxystearate esters of ethoxylated glycerol with small amounts of macrogol hydroxystearate and the corresponding free glycols. Both substances are generally highly dispersible in water.

The aim of this work was to study the potential of different emulsifiers in the development of food microemulsions, evaluating their physicochemical properties. Different mixtures of sunflower oil, water, a surfactant (Kolliphor RH40 or Kolliphor ELP) and ethanol as cosurfactant were prepared to determine formulations corresponding to microemulsions. The physicochemical characteristics of the microemulsions were investigated by rheological measurements, turbidity, electrical conductivity and droplet size distribution.

2. Materials and methods

2.1. Materials

Surfactants derived from castor oil were kindly supplied by BASF Argentina S.A. (Argentina): macrogolglycerol hydroxystearate (Kolliphor RH40) and macrogolglycerol ricinoleate (Kolliphor ELP). Commercial sunflower oil was purchased from Molinos Cañuelas (SACIFIA, Argentina) and used without additional purification. Analytical grade ethanol > 99.5% was used as cosurfactant (Soria, Argentina). Sodium azide was used as antimicrobial agent (Anedra, Argentina). Distilled and deionized water was added to all microemulsions.

2.2. Methods

2.2.1. Construction of phase diagrams

Initially, mixtures of surfactant (Kolliphor RH40 or Kolliphor ELP), sunflower oil and cosurfactant (absolute ethanol) were prepared by magnetic stirring to ensure the correct homogenization of these components, using a temperature controlled bath at 40 °C. Different proportions between emulsifier and oil/ethanol were studied (9:1, 8:2, 7:3, 6:4, 5:5, 4:6, 3:7, 2:8 and 1:9), keeping a constant ratio of sunflower oil: ethanol (2:1). Subsequently, distilled water was added constantly stirring at 350 rpm. Finally, each formulation was placed in a sonicator bath for 1 h at 40 °C to remove occluded bubbles.

Systems were named according to their formulation; i.e., first numbers corresponded to the surfactant concentration in the oil phase, then the letters indicated the type of emulsifier ("RH" for Kolliphor RH40 and "ELP" for Kolliphor ELP), and final numbers represented the final water concentration in the system. For example, a system named 90RH80 consisted of an emulsion with 80 g water/100 g emulsion, using an oil phase with 90 g surfactant/100 g organic phase (9:1 ratio) of Kolliphor RH40: (oil + ethanol). Particularly, Line 8 (L8) corresponds to the mixture of surfactant 80% and oil + cosurfactant 20%, and Line 9 (L9) corresponds to the mixture of surfactant 90% and oil + cosurfactant 10%.

All formulations were performed at least in duplicate and stored at 20 °C for one month. Those which remained stable were subjected to 60 °C for two days prior to the construction of the pseudo-ternary phase diagram.

2.2.2. Characterization of the pseudo-ternary phase diagrams

The various formulations were visually observed to construct the pseudo-ternary phase diagram. Those systems consisting of separated oily and aqueous phases were classified as "two phases" (2P), while white single-phase systems were named as "emulsions" (E). On the other hand, those systems that after the storage period still remained as a single transparent and colorless phase were classified as "microemulsions" (ME).

2.2.3. Storage stability

The stability of samples was investigated by absorbance measurements using a spectrophotometer (Hach DR2800). All prepared samples were stored for 34 days at 20 °C and their absorbance was regularly measured at a wavelength of 500 nm (Pearce & Kinsella, 1978). Then, only those systems that remained stable were subjected to an accelerated destabilization process in an oven at 60 °C for 48 h, followed by a final measure of the absorbance. The results were expressed as turbidity variation (τ), calculated according to:

$$\Delta\tau\ (\mathrm{cm}^{-1}) = \tau(t) - \tau(0) \quad (1)$$

where: $\tau(t) = \frac{2.303 abs(t)}{l}$ is the turbidity at time "t", τ(0) the initial turbidity, *abs* is the measured absorbance and *l* the optical path of the cell (Cho, Kim, Bae, Mok, & Park, 2008).

2.2.4. Conductivity measurement

Conductivity measurements were performed in order to classify the microemulsions as oil in water (O/W) or water in oil (W/O). The conductivity was determined using a conductivity meter (Lutron, CD-4307SD). The measurements were carried out in duplicate and the temperature was kept constant at 25 °C.

2.2.5. Droplets size distribution

Dynamic light scattering equipment (Horiba SZ-100, Horiba Scientific, Japan) was used to evaluate the droplet size distribution and the mean hydrodynamic diameter of the fluid o/w microemulsions obtained with both emulsifiers. All microemulsions were measured in duplicate and 10 measurements were performed on each cell, reporting the average value in each case.

2.2.6. Rheological measurements

Oscillatory and rotational rheological tests were carried out on a Haake RS600 controlled stress rheometer (Haake, Germany). All measurements were performed at least in duplicate and maintaining a constant temperature of 25 °C. Parallel plates of 60 mm diameter or double gap concentric cylinders were used depending on the viscosity of the analyzed sample.

2.2.6.1. Oscillatory tests. Stress sweeps were performed at a fixed oscillation frequency of 1 Hz (6.28 rad/s) to determine the linear viscoelastic range (LVR). Afterwards, within the LVR, frequency sweeps were carried out to determine the variation of the elastic (G′) and viscous (G″) moduli within the range 0.01–100 rad/s.

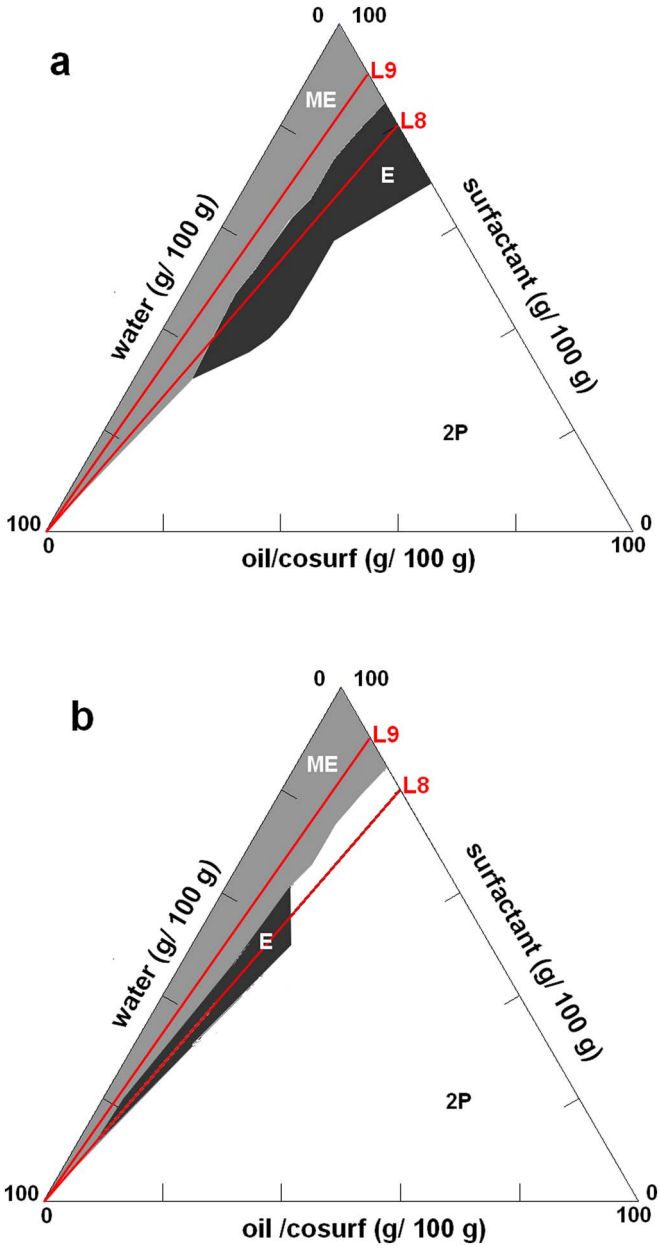

Fig. 1. Pseudo-ternary phase diagrams for systems emulsified with (a) Kolliphor RH40, (b) Kolliphor ELP. The lines L9 and L8 correspond to the ratio 9:1 and 8:2 of surfactant: (oil + cosurfactant), respectively. ME: microemulsion, E: emulsion, 2P: two phases.

2.2.6.2. Steady state flow measurement. The flow measurements were obtained by imposing a ramp of shear stresses and waiting until the slope of the resulting shear rate versus time was < 0.001% at each point, so that it could be assumed that steady-state was almost attained (Lorenzo, Zaritzky, & Califano, 2008).

2.2.7. Statistical analysis

Analyses of variance were conducted separately on the dependent variables analyzed. Tukey's test was chosen for simultaneous pairwise comparisons. Differences in means and F-tests were considered statistically significant when $P < 0.05$. All statistical procedures were computed using the SYSTAT software (SYSTAT Inc., Evanston, IL, USA).

3. Results and discussion

3.1. Phase diagram analysis

The pseudo-ternary phase diagrams were constructed from the visual observation for systems containing Kolliphor RH40 (Fig. 1a) and Kolliphor ELP (Fig. 1b). Regardless of the type of the emulsifier, microemulsions could only be obtained with emulsifier: (oil + ethanol) ratios higher than 7:3. Lowering surfactant concentration in the oil phase, led to a region where turbid macroemulsions were produced, but using ratios lower than 6:4 systems become unstable with rapid phase separation. Similar behavior was observed by different authors using other nonionic emulsifiers (Fasolin et al., 2012; Roohinejad et al., 2015) or lecithin (Abbasi & Radi, 2016). Fig. 1 shows that the emulsifier Kolliphor RH40 presented a larger region of micro-emulsified systems than that obtained with Kolliphor ELP. This would result in greater variation in the compositions to produce stable colloidal systems.

Fig. 2 presents photographs of different pseudo-ternary systems, elaborated with Kolliphor RH40 and Kolliphor ELP, corresponding to different regions of the diagram.

3.2. Stability test

The stability of the systems was determined during 34 days of storage at 20 °C from turbidity measurements. Line 9 (L9) systems formulated with Kolliphor RH40 and Kolliphor ELP showed very low constant turbidity values throughout the storage which can be associated with high stability for all water concentrations. Fig. 2 shows the transparency of these systems that practically did not differentiate from pure water. On the other hand, Fig. 3a shows variation of turbidity with storage time for some systems of Line 8 (L8). Systems of L8 with 80% and 60% water prepared with Kolliphor RH40 (i.e., 80RH80 and 80RH60) presented values of $\Delta\tau$ very close to zero, since they behaved as microemulsions. Those systems that resulted in emulsions (80RH20, 80ELP80 and 80ELP60) showed negative values of $\Delta\tau$ due to the destabilization process. This is associated with the creaming of the oil droplets. When they begin to move towards the top of the tube, the lower zone is clarified giving a decrease in turbidity (Quintana, Lorenzo, Zaritzky, & Califano, 2007). The $\Delta\tau$ of these samples presented a marked initial decay that was later decelerated with storage. However, the 80ELP20 sample showed very large destabilization kinetics throughout the period leading to phase separation (Fig. 3a).

After storage at 20 °C, systems that did not show changes in turbidity were subjected to an accelerated destabilization process heating the samples at 60 °C for 48 h. By turbidity measurements, it was determined that there were no significant changes in these formulations, which ended up defining them as microemulsions.

3.3. Droplets size distribution

The droplets size distribution and the average size of droplets were determined on the microemulsions obtained with different emulsifiers. All microemulsions showed a monomodal distribution with a low polydispersity index (< 0.30) and an average droplet size below 20 nm (Table 1); as an example Fig. 3b shows the droplet size distribution for some of the studied formulations.

In none of the cases studied the total dispersed phase content affected the droplet size or its distribution. However, it was observed that as the emulsifier: (oil + cosurfactant) ratio decreased, the drops showed a significant size increase. With the gradual addition of oil to the disperse phase, i.e., a decrease in the ratio, micelles are swollen by oil and consequently the droplet size of the microemulsion is also gradually increasing. This behavior was also reported by other authors in microemulsions of water-in- ionic liquids using TX-100 as emulsifier (Seth, Chakraborty, Setua, & Sarkar, 2007). Besides, microemulsions made with Kolliphor ELP presented a hydrodynamic droplet size

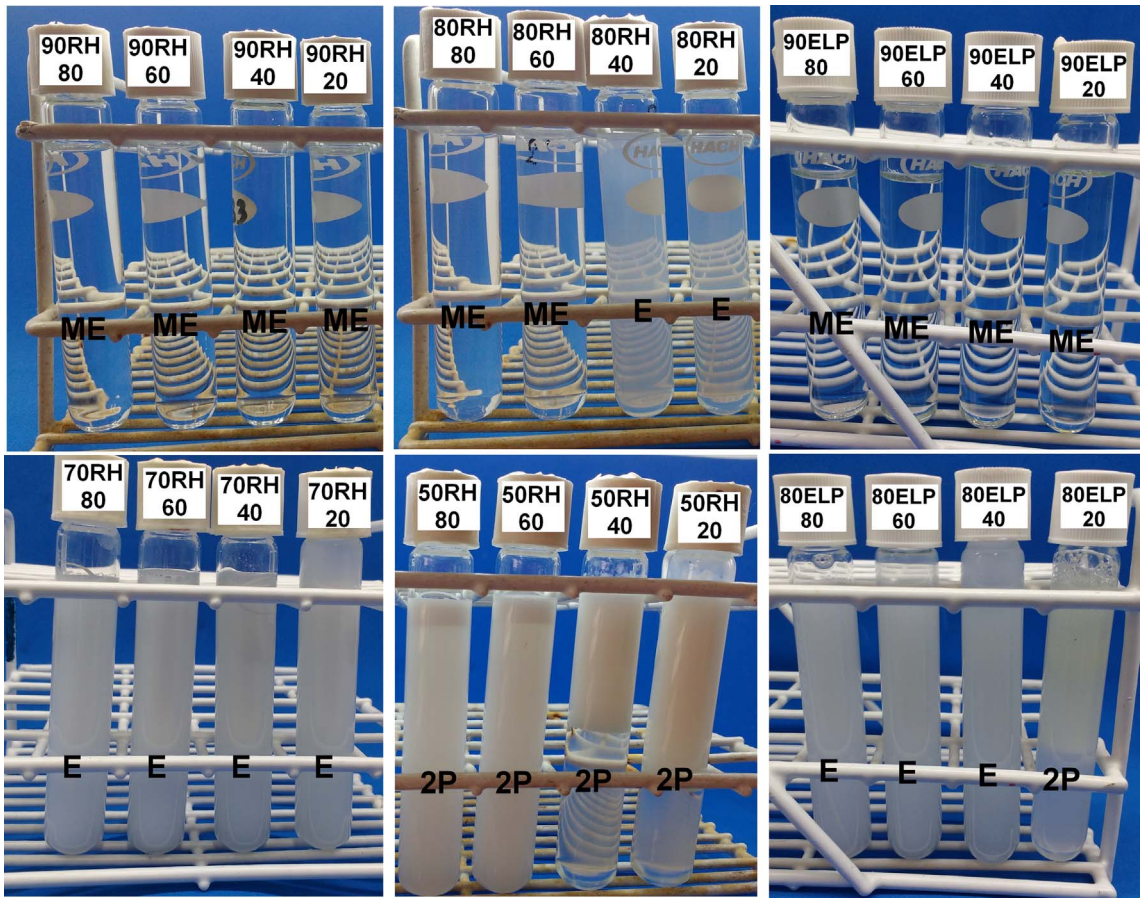

Fig. 2. Photographs corresponding to systems of different zones of the phase diagram, elaborated with Kolliphor RH40 and Kolliphor ELP. Microemulsions (ME), emulsion (E), and two phases (2P).

significantly ($P < 0.05$) smaller than those elaborated with Kolliphor RH40. This effect could be attributed to the difference in the chain length of the emulsifiers. Chain length of polyethylene glycol (PEG) castor oils and PEG hydrogenated castor oils depends on the quantity of ethylene oxide used in synthesis (Fruijtier-Pölloth, 2005), so it was expected a larger hydrodynamic diameter for microemulsions containing RH40.

3.4. Electric conductivity

Conductivity measurements were carried out for Line 8 and 9 microemulsions formulated with Kolliphor RH40 and ELP. However, not all systems could be studied due to their gel-like behavior. A similar behavior was observed for the two emulsifiers, with two well defined conductivity zones as shown in Fig. 3c. At low water concentrations, very low conductivity values were obtained associated with the low conductivity of the oil and the large amount of non-ionic emulsifier. These systems were classified as water-in-oil microemulsions. As the concentration of the polar phase increase, a sharp increment in the conductivity was observed. Several authors have reported this phenomenon as the percolation threshold, where the swollen micelles start interacting each other (Kumar & Mittal, 1999; Ma & Zhong, 2015). For water concentrations higher than 60 g/100 g emulsion, there was a marked increase in conductivity up to 70 g/100 g emulsion that could be attributed to the transition of W/O microemulsions to bicontinuous structure. After further dilution to > 70 g water/100 g emulsion, the bicontinuous structure shifts to O/W microemulsions. Fasolin et al. (2012) informed an analogous performance working with systems prepared with sunflower oil or high oleic sunflower oil, water, Tween 80, and ethanol. Ma and Zhong (2015) registered similar concentrations for the transition in microemulsions with soybean oil, using different essential oils, and Tween 80.

3.5. Viscoelastic behavior of microemulsions

Stress sweeps of the different microemulsions were carried out to determine their linear viscoelastic range. Fig. 4a shows the complex modulus ($G^* = ((G')^2 + (G'')^2)^{1/2}$) as a function of the stress amplitude for some of the formulations tested. All microemulsions were invariant throughout the range of stresses measured even with high dispersed phase contents such as 90RH40 emulsions (60% oil + emulsifier + cosurfactant). Based on this, it was adopted a stress of 1 Pa to perform the frequency sweeps.

Subsequently, frequency sweeps were obtained for the microemulsions. Fig. 4b shows the elastic modulus (G′) and the viscous modulus (G″) as a function of frequency for the microemulsions of line 9. Those with higher water content (90RH80, 90RH60) showed a marked viscous behavior similar to a dilute solution, with very low values of G′ and G″ and a marked linear dependence with frequency throughout the studied range. G″ was higher than G′ but with a tendency to show a crossover at frequency higher than 10^2 rad/s. Based on this trend it could be made a rough estimation of the relaxation time ($\lambda = 1/\omega_{crossover}$) of the microemulsions which was lower than 10^{-2} s, an indicator of the extremely low elasticity of this system (Tadros, 1996). A similar viscoelastic behavior was observed in those microemulsions obtained with Kolliphor ELP. On the other hand, microemulsions containing 60 g dispersed phase/100 g emulsion (90RH40) showed a weak gel-like behavior with G′ values higher than G″ over a wide frequency range, with a minimum of the latter at intermediate frequencies and a "plateau" region in G′ (Steffe, 1996). A marked decrease in the

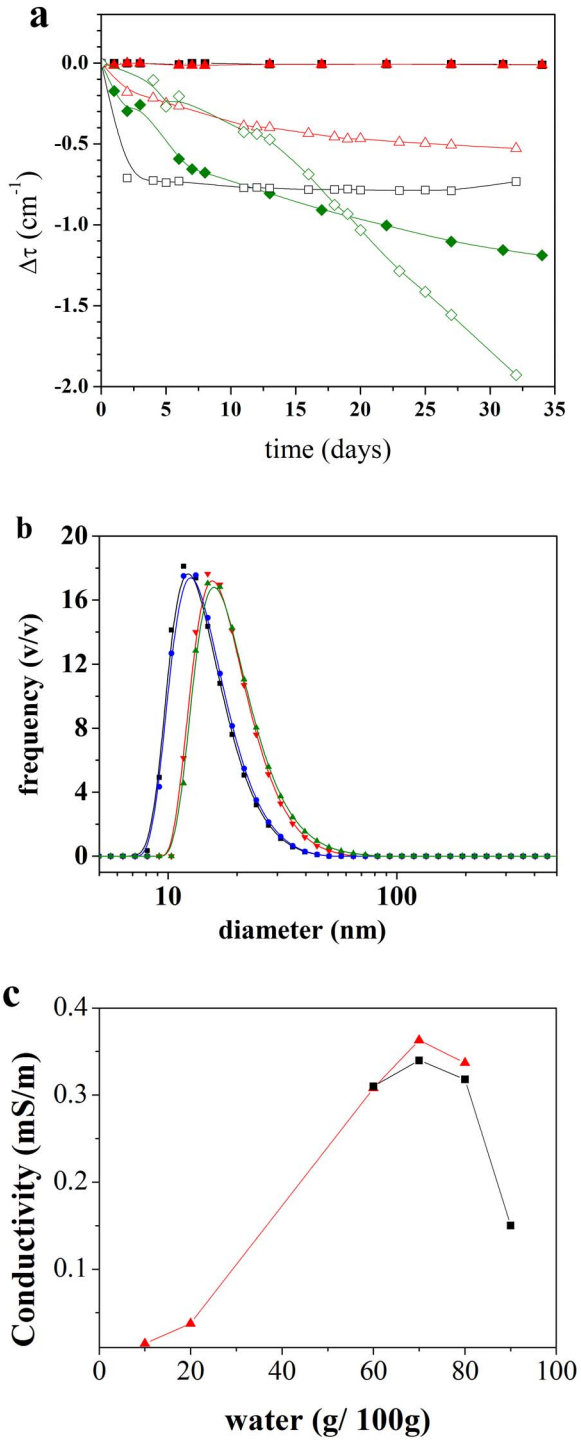

Fig. 3. a) Variation of turbidity as a function of storage time at 20 °C for Line 8 systems: ■80RH80, □80ELP80, ▲80RH60, △80ELP60, ◆80RH20, ◇80ELP20. b) Droplet size distribution for microemulsions formulated with Kolliphor RH40 with different concentrations of water and emulsifier: (oil + ethanol) ratios. 80RH60 (▲), 80RH80 (▼), 90RH60 (■), 90RH80 (●). c) Conductivity of microemulsions formulated with Kolliphor RH40 as a function of water content using ratios 9:1 (▲) and 8:2 (■) for emulsifier: (oil + ethanol).

crossover frequency was observed in this formulation (a major increase in relaxation time was observed when gum concentration reached 1.25% ($\omega_{crossover} \sim 3.10^{-2}$ rad/s), which is related with a major increment in the elastic behavior and strength of the structure. Significant differences between microemulsions can also be observed in the photographs of Fig. 4a. Increasing fraction of the dispersed organic phase

Table 1
Average droplet size (nm) and polydispersity index for stable microemulsions formulated with an oil phase with 80 or 90 g surfactant/100 g organic phase and Kolliphor RH or Kolliphor ELP as surfactants.*

Formulation	Average droplet size (nm)+	Polydispersity index+
80RH60	18.38^{a} (1.62)	0.283^{a} ($2.8 \cdot 10^{-2}$)
80RH80	18.46^{a} (0.155)	0.293^{a} ($7.7 \cdot 10^{-3}$)
90RH60	14.26^{b} (0.236)	0.217^{b} ($2.1 \cdot 10^{-2}$)
90RH80	14.46^{b} (1.27)	0.225^{b} ($6.7 \cdot 10^{-3}$)
90ELP60	12.77^{c} (0.255)	0.205^{b} ($3.8 \cdot 10^{-3}$)
90ELP80	11.78^{c} (0.075)	0.183^{b} ($6.0 \cdot 10^{-3}$)

* SEM is given between parentheses.
+ Different superscripts within the same column indicate significant differences ($P < 0.05$).

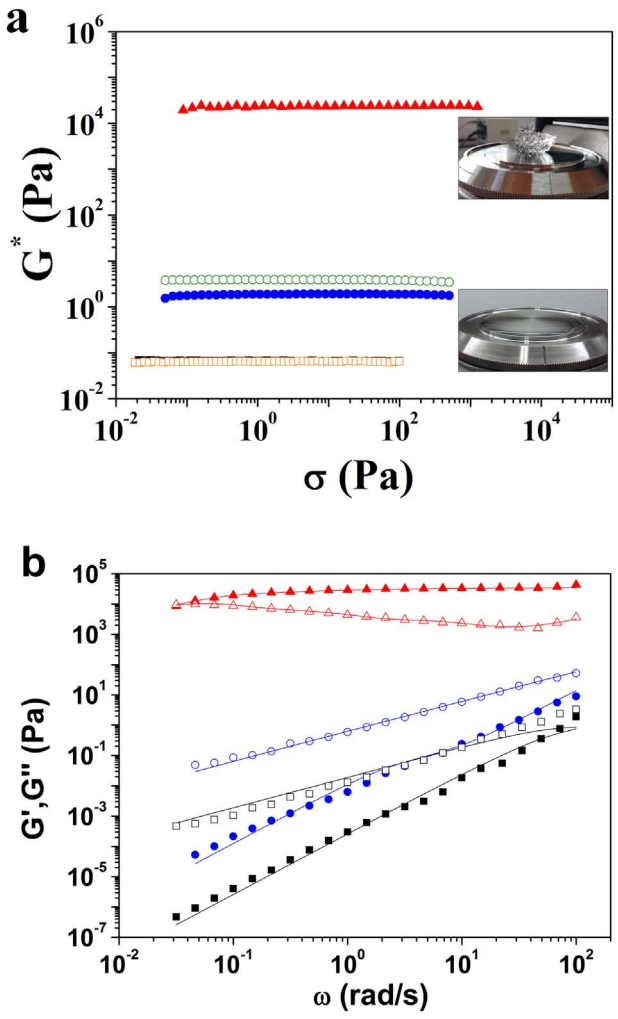

Fig. 4. Oscillatory rheology for microemulsions stabilized with Kolliphor RH40. a) Stress sweeps for 90RH80 (■), 90RH60 (●), 90RH40 (▲), 80RH80 (□), and 80RH60 (○). Insert pictures correspond to 90RH80 (down) and 90RH40 (up). b) Frequency sweeps for 90RH80 (■ □), 90RH60 (● ○), and 90RH40 (▲ △). Full symbols: G′; empty symbols: G″. Continuous lines: Maxwell model.

led to a transition from o/w microemulsion to a bicontinuous structure, which is revealed by the strengthened interaction between dispersed domains of the oily phase (Garti, Yaghmur, Leser, Clement, & Watzke, 2001).

Fig. 4b also shows the fitting of the discrete generalized Maxwell model for microemulsions of line 9. Parameters of the model (number of elements, N, elastic modulus of each element, Gi, and each relaxation time, λi) were determined using a non-linear numerical method

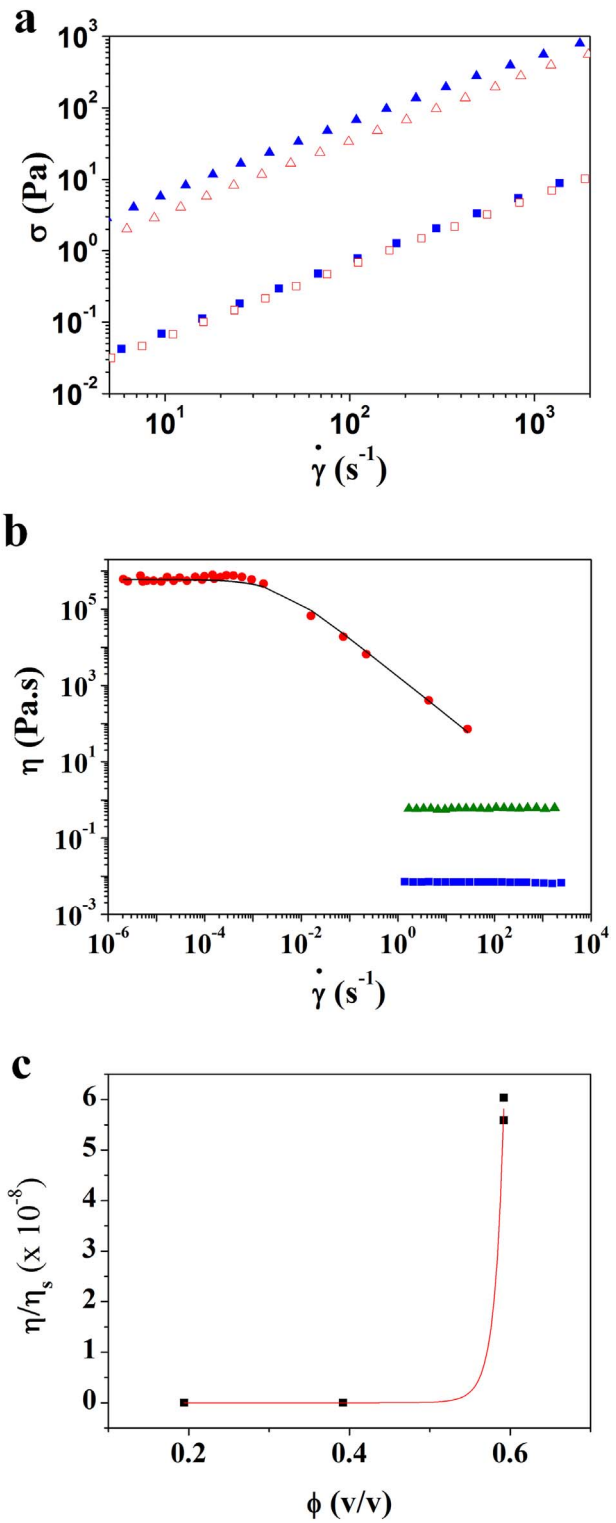

Fig. 5. a) Shear stress (σ) vs. shear rate ($\dot{\gamma}$) for microemulsions with Kolliphor RH40: 80RH60 (△), 80RH80 (□), 90RH60 (▲), and 90RH80 (■). b) Flow curves for microemulsions of line 9 with 20 (■), 40 (▲) and 60% (●) dispersed phase. Continuous line: Cross model. c) Relative viscosity (η/η_s) as a function of dispersed phase fraction (ϕ). Continuous line: Dougherty-Krieger model.

previously described (Lorenzo, Zaritzky, & Califano, 2015; Winter & Mours, 2006). The computed Gi and λi values were used to predict the storage and loss moduli. As can be observed in Fig. 4b, there is a satisfactory agreement between the experimental and predicted values, confirming the accuracy of the calculations. Once the relaxation time spectrum was known other material functions such as the plateau modulus G_0^N were evaluated as the sum of the relaxation moduli (Mead, 1994). Increasing disperse content was correlated with a significant increment in G_0^N values. This parameter was previously related to the number of entanglements between wormlike micelles, or, the mesh size of the network (Lorenzo et al., 2015; Sharma et al., 2009). Thus, the increase in G_0^N with increasing ϕ could be attributed to an increase in the network density of the droplets surrounded with wormlike micelles.

3.6. Flow behavior of the microemulsions

Fig. 5a shows the dependence of shear stress with shear rate for 90RH80, 90RH60, 80RH80 and 80RH60 microemulsions. The shear curves invariably showed Newtonian behavior over the shear range studied and in no samples could a yield stress be detected. The linearity of the flow curves for these microemulsions could be observed over at least 3 orders of magnitude of σ (Fig. 5a). This is a usual behavior observed in microemulsions as reported by different authors (Fasolin et al., 2012; Špiclin, Homar, Zupančič-Valant, & Gašperlin, 2003).

Both the variation in emulsifier or water contents showed an influence on the flow behavior. Regardless the emulsifier concentration, systems containing 60 g water/100 g had higher viscosity ($\eta \sim 4 \times 10^{-1}$ Pa·s) than those containing 80 g/100 g ($\eta \sim 6 \times 10^{-3}$ Pa·s). A decrease in the water content involves an increase in dispersed phase concentration of the O/W microemulsions, and hence an increase in the number of droplets, which enhance the interaction between them and consequently the viscosity. When the dispersed phase content was 20 g/100 g, no influence of the emulsifier: (oil + ethanol) ratio was observed. Conversely, when this content increased to 40 g/100 g, those microemulsions with the highest concentration of Kolliphor RH40 (line 9) showed significant higher viscosities ($\eta = 4.84 \times 10^{-1} \pm 9.6 \times 10^{-3}$ Pa·s) than those of line 8 ($\eta = 2.70 \times 10^{-1} \pm 6.7 \times 10^{-3}$ Pa·s).

When the dispersed phase content was increased to 60 g/100 g a marked change in flow properties was observed as seen in Fig. 5b. The microemulsions showed a characteristic pseudoplastic behavior with a constant viscosity below 10^{-3} s^{-1} and a sharp decrease at higher shear rates. This behavior was described using the Cross model (Steffe, 1996):

$$\eta = \frac{\eta_0}{(1 + (\tau\dot{\gamma})^n)} \quad (2)$$

where η is the viscosity corresponding to a shear rate $\dot{\gamma}$, η_0 is the viscosity at $\dot{\gamma} = 0$; τ is a relaxation time, and n a measure of the pseudoplastic characteristics.

The satisfactory agreement between Cross model and rheological data could be observed in Fig. 5b. This is a typical behavior reported in lipogels and gel microemulsion generally used in drug delivery matrices for topical application (Ellaithy & El-Shaboury, 2002). At rest, molecules and droplets remain entangled together with the association of immobilized aqueous phase. Once the shear rate increases enough, emulsifier molecules tend to disentangled and droplets align in the direction of flow, offering less resistance. This together with the release of some of the entrapped water accounts for the decrease in the viscosity.

There are several models to interpret the viscosity variation of emulsions with the volume fraction of disperse phase (ϕ).Considering that droplets of the microemulsion have a net charge close to zero because they are surrounded with a nonionic emulsifier, they will only interact by excluded volume effects. Under these conditions it is possible to apply the Dougherty-Krieger model developed for hard sphere systems (Rao, 2013):

$$\frac{\eta}{\eta_s} = \left(1 - \frac{\phi}{\phi_m}\right)^{-[\eta]\phi_m} \quad (3)$$

where η_s is the viscosity of the continuous phase, ϕ is the dispersed phase volume fraction, ϕ_m is the maximum packaging fraction, and [η]

is the intrinsic viscosity of the microemulsion.

As shown in Fig. 5c, Eq. (3) satisfactorily fitted the experimental data obtaining ϕ_m and [η] values of 0.72 and 16.24, respectively. The predicted ϕ_m was > 0.63 which is usually obtained for randomly packed uniform hard spheres. On the other hand $\phi_m = 0.74$ corresponds to closest packing, a face-centered cubic array. Other authors reported similar values of ϕ_m that can be attributed to systems that can be densely packed and achieve a high ordering of their structure (Chen & Warr, 1992).

4. Conclusion

Emulsifiers derived from castor oil resulted in a useful alternative to produce different types of microemulsions. Particularly, polyoxyl 40 hydrogenated castor oil (Kolliphor RH40), allowed working with higher concentrations of oil than Kolliphor ELP. Systems were very stable during storage and temperature changes, showing droplet sizes within the colloidal domain, lower than 20 nm. It was observed that the systems with higher water content presented a Newtonian behavior, which would indicate the existence of very small droplets separated enough to be able to interact with each other. Increasing the dispersed phase content produced a weak gel-like structure with pseudoplastic behavior under flow conditions that could be satisfactorily modeled to obtain structural parameters.

Acknowledgements

The authors are grateful to BASF Argentina S.A., who provided the emulsifiers for this study. The financial support of the Consejo Nacional de Investigaciones Científicas y Técnicas (CONICET) (PIP 0546), Agencia Nacional de Promoción Científica y Tecnológica (PICT 2015-0344) and Universidad Nacional de La Plata (X728) is also acknowledged.

References

Abbasi, S., & Radi, M. (2016). Food grade microemulsion systems: Canola oil/lecithin:N-propanol/water. *Food Chemistry, 194*, 972–979.

Berthelsen, R., Holm, R., Jacobsen, J., Kristensen, J., Abrahamsson, B., & Müllertz, A. (2015). Kolliphor surfactants affect solubilization and bioavailability of fenofibrate. Studies of in vitro digestion and absorption in rats. *Molecular Pharmaceutics, 12*(4), 1062–1071.

Callender, S. P., Mathews, J. A., Kobernyk, K., & Wettig, S. D. (2017). Microemulsion utility in pharmaceuticals: Implications for multi-drug delivery. *International Journal of Pharmaceutics, 526*(1), 425–442.

Chen, C. M., & Warr, G. G. (1992). Rheology of ternary microemulsions. *The Journal of Physical Chemistry, 96*(23), 9492–9497.

Cho, Y. H., Kim, S., Bae, E. K., Mok, C., & Park, J. (2008). Formulation of a cosurfactant-free O/W microemulsion using nonionic surfactant mixtures. *Journal of Food Science, 73*(3), 115–121.

Ellaithy, H., & El-Shaboury, K. (2002). The development of cutina lipogels and gel microemulsion for topical administration of fluconazole. *AAPS PharmSciTech, 3*(4), 77–85.

El-Sayed, H. S., Chizzola, R., Ramadan, A. A., & Edris, A. E. (2017). Chemical composition and antimicrobial activity of garlic essential oils evaluated in organic solvent, emulsifying, and self-microemulsifying water based delivery systems. *Food Chemistry, 221*, 196–204.

Fasolin, L. H., Santana, R., & Cunha, R. (2012). Microemulsions and liquid crystalline formulated with triacylglycerols: Effect of ethanol and oil unsaturation. *Colloids and Surfaces A: Physicochemical and Engineering Aspects, 415*, 31–40.

FDA (2017). Food and Drug Administration. Inactive ingredient for approved drug products. Retrieved from https://www.accessdata.fda.gov/scripts/cder/iig/index.cfm?event=browseByLetter.page&Letter=P.

Flanagan, J., & Singh, H. (2006). Microemulsions: A potential delivery system for bioactives in food. *Critical Reviews in Food Science and Nutrition, 46*(3), 221–237.

Fruijtier-Pölloth, C. (2005). Safety assessment on polyethylene glycols (Pegs) and their derivatives as used in cosmetic products. *Toxicology, 214*(1), 1–38.

Garg, T., Sharma, G., Rath, G., & Goyal, A. K. (2017). 18 - Colloidal systems: An excellent carrier for nutrient delivery. In A. M. Grumezescu (Ed.). *Nutrient delivery* (pp. 681–712). Academic Press.

Garti, N., & Aserin, A. (2012). 9 - Micelles and microemulsions as food ingredient and nutraceutical delivery systems. In N. Garti, & D. J. McClements (Eds.). *Encapsulation technologies and delivery systems for food ingredients and nutraceuticals* (pp. 211–251). Woodhead Publishing.

Garti, N., Yaghmur, A., Leser, M. E., Clement, V., & Watzke, H. J. (2001). Improved oil solubilization in oil/water food grade microemulsions in the presence of polyols and ethanol. *Journal of Agricultural and Food Chemistry, 49*(5), 2552–2562.

Hallouard, F., Dollo, G., Brandhonneur, N., Grasset, F., & Corre, P. L. (2015). Preparation and characterization of spironolactone-loaded nano-emulsions for extemporaneous applications. *International Journal of Pharmaceutics, 478*(1), 193–201.

Janković, J., Djekic, L., Dobričić, V., & Primorac, M. (2016). Evaluation of critical formulation parameters in design and differentiation of self-microemulsifying drug delivery systems (SMEDDSS) for oral delivery of aciclovir. *International Journal of Pharmaceutics, 497*(1), 301–311.

Kumar, P., & Mittal, K. L. (1999). *Handbook of microemulsion science and technology.* CRC Press.

Li, Y., Yokoyama, W., Xu, S., Zhu, S., Ma, J., & Zhong, F. (2017). Formation and stability of W/O microemulsion formed by food grade ingredients and its oral delivery of insulin in mice. *Journal of Functional Foods, 30*, 134–141.

Lorenzo, G., Zaritzky, N., & Califano, A. (2008). Modeling rheological properties of low-in-fat O/W emulsions stabilized with xanthan/guar mixtures. *Food Research International, 41*(5), 487–494.

Lorenzo, G., Zaritzky, N., & Califano, A. (2015). Mechanical and optical characterization of gelled matrices during storage. *Carbohydrate Polymers, 117*, 825–835.

Lv, F.-F., Zheng, L.-Q., & Tung, C.-H. (2005). Phase behavior of the microemulsions and the stability of the chloramphenicol in the microemulsion-based ocular drug delivery system. *International Journal of Pharmaceutics, 301*(1), 237–246.

Ma, Q., & Zhong, Q. (2015). Incorporation of soybean oil improves the dilutability of essential oil microemulsions. *Food Research International, 71*, 118–125.

Mead, D. (1994). Numerical interconversion of linear viscoelastic material functions. *Journal of Rheology, 38*(6), 1769–1795.

Pearce, K. N., & Kinsella, J. E. (1978). Emulsifying properties of proteins: Evaluation of a turbidimetric technique. *Journal of Agricultural and Food Chemistry, 26*(3), 716–723.

Quintana, J., Lorenzo, G., Zaritzky, N., & Califano, A. (2007). Hydrocolloids as O/W emulsion stabilizers: Effect of the structural features during storage. In C. Lupano (Ed.). *Functional properties of food components* (pp. 1–22). Research Signpost: Kerala.

Rao, A. (2013). *Rheology of fluid, semisolid, and solid foods: Principles and applications.* Springer Science & Business Media.

Roohinejad, S., Oey, I., Wen, J., Lee, S. J., Everett, D. W., & Burritt, D. J. (2015). Formulation of oil-in-water B-carotene microemulsions: Effect of oil type and fatty acid chain length. *Food Chemistry, 174*, 270–278.

Rozman, B., Zvonar, A., Falson, F., & Gasperlin, M. (2009). Temperature-sensitive microemulsion gel: An effective topical delivery system for simultaneous delivery of vitamins C and E. *AAPS PharmSciTech, 10*(1), 54–61.

Seth, D., Chakraborty, A., Setua, P., & Sarkar, N. (2007). Interaction of ionic liquid with water with variation of water content in 1-butyl-3-methyl-imidazolium hexafluorophosphate ([Bmim][Pf 6])/Tx-100/water ternary microemulsions monitored by solvent and rotational relaxation of coumarin 153 and coumarin 490. *The Journal of Chemical Physics, 126*(22), 224512.

Sharma, S. C., Shrestha, L. K., Tsuchiya, K., Sakai, K., Sakai, H., & Abe, M. (2009). Viscoelastic wormlike micelles of long polyoxyethylene chain phytosterol with lipophilic nonionic surfactant in aqueous solution. *The Journal of Physical Chemistry B, 113*(10), 3043–3050.

Špiclin, P., Homar, M., Zupančič-Valant, A., & Gašperlin, M. (2003). Sodium ascorbyl phosphate in topical microemulsions. *International Journal of Pharmaceutics, 256*(1), 65–73.

Steffe, J. F. (1996). *Rheological methods in food process engineering.* Freeman Press.

Tadros, T. F. (1996). Correlation of viscoelastic properties of stable and flocculated suspensions with their interparticle interactions. *Advances in Colloid and Interface Science, 68*, 97–200.

Warisnoicharoen, W., Lansley, A., & Lawrence, M. (2000). Nonionic oil-in-water microemulsions: The effect of oil type on phase behaviour. *International Journal of Pharmaceutics, 198*(1), 7–27.

Winter, H. H., & Mours, M. (2006). The cyber infrastructure initiative for rheology. *Rheologica Acta, 45*(4), 331–338.

Xu, Z., Jin, J., Zheng, M., Zheng, Y., Xu, X., Liu, Y., & Wang, X. (2016). Co-surfactant free microemulsions: Preparation, characterization and stability evaluation for food application. *Food Chemistry, 204*, 194–200.